



OPEN

Fine tuning enzyme activity assays for monitoring the enzymatic hydrolysis of PET

Krisztina Boros, Blanka Eszter Nagy, Raluca Bianca Tomoiagă, Róbert Tőtős, Monica Ioana Toşa, Csaba Paizs & László Csaba Bencze✉

Efficient monitoring of the enzymatic PET-hydrolysis is crucial for developing novel plastic-degrading biocatalysts. Herein, we aimed to upgrade in terms of accuracy the analytical methods useful for monitoring enzymatic PET-degradation. For the HPLC-based assessment, the incorporation of an internal standard within the analytic procedure enabled a more accurate quantification of the overall TPA content and the assessment of molar distributions and relative content of each aromatic degradation product. The provided calibration curves cover a broad concentration range, from μM to low mM scale, facilitating assessment of both lower and higher PETase activities, with a limit of detection positioned below the reported PET-degrading activities. The increased reproducibility and accuracy of the improved HPLC method, compared to the previous methods, was supported by lower dispersion of product concentrations and their lower deviation from theoretical values over multiple measurements. The other predominantly employed UV-spectroscopy assay was also improved in terms of employed wavelength and medium extinction coefficient of the three aromatic degradation products, while being cross-validated by the improved HPLC method. Finally, both methods were used for monitoring the product formation within the leaf-branch compost cutinase (LCC)-mediated PET-hydrolysis and provided individual time-productivity profiles for each aromatic degradation product.

Due to its various advantageous properties, polyethylene terephthalate (PET) is one of the most widely produced polyesters^{1–3}. Considering the annual production of ~ 400 million tons of plastic in 2022, estimated to increase to ~ 1 billion tons/year in 2050, while calculating with the current recyclability rates, the amount of plastics present in landfills or in the natural environment is expected to reach 12 billion tons by 2050^{2–7}, representing a major, global environmental threat⁸. The degradation-based fragmentation of polyethylene terephthalate, induced by physical abrasion, UV light, heat and microbial action⁹, leads to PET micro- and nanoparticles that are omnipresent, being detected in surface waters, deep-sea sediments, air^{10–13}, and even human blood^{14,15}, while related toxicity issues are emergently reported¹. Considering all, the degradation, depolymerization of PET to its monomers, that, besides recycled PET, also serves for other commodities, is highly desirable. During the large-scale employed thermomechanical recycling, the decrease in PET's mechanical properties occurs, limiting the number of recycling cycles¹⁶. Through the chemical¹⁷ or enzymatic¹⁸ depolymerisation, the chemical building blocks from the PET waste can be recovered, which can replace virgin monomers during their (re)polymerisation into PET. The process aligns with the concept of circular economy and decreases the need for the fossil-based terephthalic acid, moreover the obtained monomers and/or dimers, trimers, besides (re)polymerisation, can possess additional valorisation possibilities¹⁹.

In 2005, the possibility of enzymatic hydrolysis of PET films was firstly reported²⁰, followed by further significant efforts to provide industrially feasible biocatalytic PET-depolymerization by the use of hydrolases, such as lipases, cutinases, and later PETases^{2,3,21–26}. Nevertheless, one of the main obstacles in biodegradation remained the inaccessibility of the amorphous domains of the PET polymer for the enzymatic attack. In this context, enzyme variants with improved thermal stability, operating with high activity at the glass transition temperature of PET, such as the leaf-branch compost cutinase (LCC)^{21,27}, became potent candidates for PET depolymerisation. While the biocatalytic degradation of microplastics in different environmental samples has just started to be explored²⁸, the engineered variants of LCC²⁹ are already employed within the industrial biotechnological PET depolymerisation, a back-to-monomer recycling process of CARBIOS¹⁸.

Monitoring the hydrolysis activity of PETases is also a challenging endeavour, given the necessity to quantify several major products such as terephthalic acid (TPA), 2-hydroxyethyl terephthalate (MHET), and bis(hydroxyethyl terephthalate) (BHET), along with ethylene glycol (EG) (Fig. 1)³⁰. Regarding the quantification

Enzymology and Applied Biocatalysis Research Center, Faculty of Chemistry and Chemical Engineering, Babeş-Bolyai University, Arany János Street 11, 400028 Cluj-Napoca, Romania. ✉email: laszlo.bencze@ubbcluj.ro

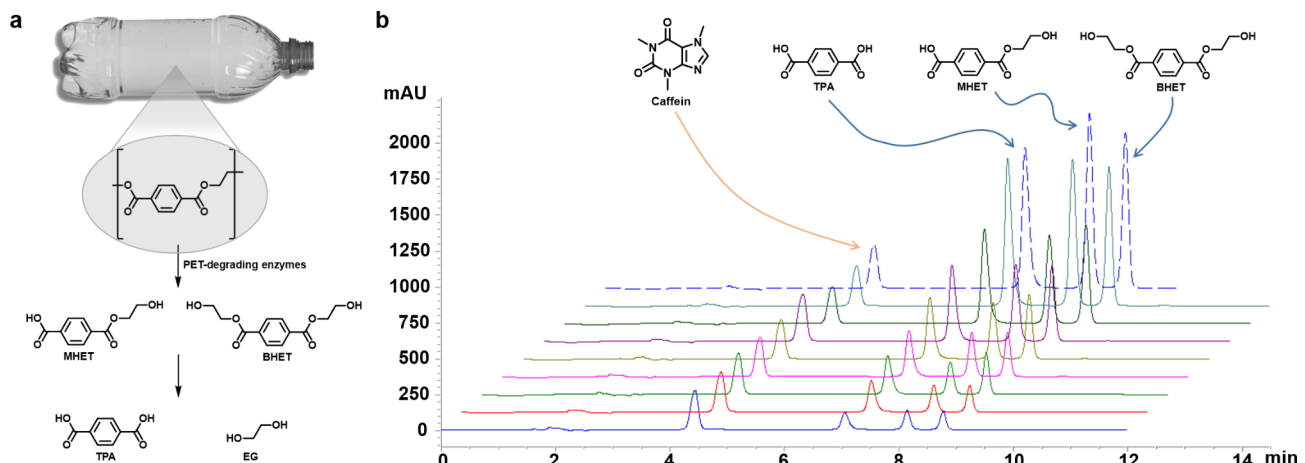


Fig. 1. Monitoring the enzymatic PET-hydrolysis: (a) The enzymatic PET-hydrolysis reaction; (b) HPLC separation of the mixtures of authentic samples containing TPA (R_T 6.4 min), MHET (R_T 7.5 min), BHET (R_T 8.1 min) at concentration range from 0.176 to 1.69 mM and the internal standard (caffeine) (R_T 4 min) at constant 2.11 mM concentration.

of EG, colorimetric methods are included in the US Pharmacopeia³¹, while gas- or liquid-chromatography techniques have also been developed based on the analysis of the benzoyl chloride-derivatized ethylene glycol^{32–34}. The detection and quantification of PET-degradation products, by fluorimetric^{30,35} and pH-based colorimetric methods^{30,36}, is limited to TPA detection, which is not in all cases the predominant product of hydrolysis. The isothermal calorimetry titration method measures the heat liberated during the cleavage of the ester bond, allowing the real-time monitoring of the enzymatic PET-hydrolysis³⁷, while being more suitable for kinetic measurements. Thus, for facile activity or conversion measurements of the enzymatic PET-degradation, predominantly UV-spectroscopy or HPLC methods are used^{2,3,21,26,29,38–41}. In case of the bulk absorbance method⁴¹, linear absorbance profiles were established only for TPA and MHET at 260 nm and the quantitative determination of the total product is provided by an 1.3-fold under- or overestimation if using the extinction coefficients either for MHET or for TPA, respectively. Several published HPLC methods monitor the overall TPA content (including, besides TPA, also the contents of MHET and BHET as TPA equivalents – TPA_{eq}) of the reaction mixture, quantified by calibration curves based on the integration of peak area, corresponding to the three different aromatic degradation products^{20,25,27}.

Within this study, we focused on improving the analytical methods used for the enzymatic PET-degradation activity assessment. The HPLC method was improved by using an internal standard and provided increased accuracy for the determination of the overall TPA content. This upgraded method allows the assessment of the molar percentage of each aromatic degradation product within the reaction mixture as well. Improvements for the bulk absorbance method have been also approached, while both optimized assays were validated and compared to the reported procedures in terms of reproducibility and accuracy. Finally, the applicability of the refined methods for monitoring the enzymatic PET-degradation was tested by assessing the product formation within the LCC-mediated PET-hydrolysis. By improving the activity assessment of PET-degrading enzymes, their performance-based comparison and selection are also facilitated, which enables precise selection of the optimal biocatalyst for a specific application of the PET-hydrolysis reaction.

Experimental part

Materials

The standard commercial chemicals and solvents were obtained from Sigma Aldrich or Alfa-Aesar. The PET film, bis-(2-hydroxyethyl) terephthalate (BHET) and tris(hydroxymethyl)aminomethane (TRIS) were purchased from Sigma-Aldrich (USA). Terephthalic acid (TPA) was purchased from Alfa Aesar, while mono-(2-hydroxyethyl) terephthalic acid (MHET) was synthesized following the reported procedure⁴⁰. HPLC-grade solvents were purchased from Promochem LGC Standards (Germany). The gene encoding LCC, codon-optimized for expression in *E. coli* cells (Sect. 1 in Supplementary information) were synthesized by GenScript Biotech (The Netherlands). UV-Vis measurements were performed on an Agilent 8453 UV-vis spectrophotometer and/or BioTek Epoch 2 microplate reader, using 96-well UV-Microtiter microplates. Enzymatic PET-hydrolysis reactions were carried out in an Eppendorf ThermoMixer C, while HPLC analysis of reaction samples was conducted on an Agilent 1200 instrument.

Methods

Molecular cloning and recombinant expression

The gene encoding LCC (GenBank ID: HQ704839.1, UniProt ID: G9BY57), purchased in its codon-optimized form (Supplementary Table S1) from GenScript Biotech (The Netherlands), was cloned into pET-21a(+) vector, and was expressed in *E. coli* Rosetta (DE3) pLysS, while the N-terminal His₁₀-tagged LCC was isolated using previously reported procedures^{21,26,29,38–41} (for details see Sect. 2 in Supplementary Information).

HPLC method development

For the separation of the aromatic products of the enzymatic PET-degradation reaction (TPA, MHET, BHET) and the internal standard caffeine (Fig. 1 and Supplementary Fig. S4) several reverse-phase HPLC methods were tested. The optimal baseline separation was provided by the use of Phenomenex Luna C8(2) 5 µm, 4.6 × 150 mm column, with a gradient elution using water (0.1% formic acid) and acetonitrile with 15 vol% to 27.5 vol% increase of acetonitrile (MeCN) in 10 min, at a flow-rate of 1 mL/min, with 240 nm as detection wavelength.

HPLC calibration for quantitative assessments The calibration curves were prepared using several mixtures (> 10 samples) with variable concentrations (covering a range of 0.02 to 1.7 mM—as presented in Fig. 1b and Supplementary Fig. S5) of the authentic TPA, MHET and BHET and fixed, 2.11 mM concentration of the caffeine internal standard in each calibrator sample. 5 µL of each calibrator sample was analyzed by HPLC using the developed internal standard method, while the calibration curves were generated by plotting the *ratios* of the areas of the absorbance peak of each reaction product and of caffeine against the known concentration of each product within the analyzed calibrator sample.

Enzymatic activity assessment by HPLC *Internal standard-based method:* to 180 µL of reaction sample, taken from the enzymatic PET-degradation, 180 µL acetonitrile was added, followed by centrifugal filtration (4 min, 8000 rpm, 6200 × g) using spin centrifuge columns with 0.2 µm nylon membrane. Subsequently, into the filtered sample 6 µL of 22% HCl and 60 µL of 15 mM caffeine stock solution (in MeCN) was added to a final concentration of 2.11 mM. From the obtained samples, 5 µL was subjected to HPLC analysis, in triplicate. The total TPA content (TPA, MHET and BHET) of the reaction samples, and the correlated enzyme activity was determined using the calibration curves from Section “[HPLC calibration for quantitative assessments](#)”.

HPLC analysis without internal standard—conventional method: 50 µL of reaction sample taken from the enzymatic PET-hydrolysis were quenched with 50 µL of MeCN. The solutions were filtered via centrifugation (4 min, 8000 rpm, 6200 × g), using spin centrifuge columns with 0.2 µm nylon membrane, followed by acidulation with 22% HCl (to achieve pH 1.0). The obtained samples were analysed using the HPLC method described in Section “[HPLC calibration for quantitative assessments](#)”, except omitting the use of internal standard.

Enzymatic activity assessment by UV-spectroscopy

The UV-absorbance spectra of the aromatic PET-hydrolysis products (TPA, MHET and BHET) were recorded using their 0.1 mM solutions in phosphate buffer (100 mM K₂HPO₄ – KH₂PO₄, pH 8.0) (Fig. 3a). The individual extinction coefficient for each aromatic component, TPA, MHET and BHET, was determined using absorbance measurements at 235 nm (A₂₃₅) over a concentration range from 0.03 mM to 0.3 mM in a final volume of 200 µL of phosphate buffer (Supplementary Fig. S8).

For the enzymatic activity measurements, 10 µL of the reaction mixture was diluted with phosphate buffer (pH 8.0) to a final volume of 200 µL, and the absorbance value was determined at 235 nm (or at 260 nm). In cases where the absorbance values of the samples exceeded the linear range of the absorbance measurement provided by the instrument (in our case absorbance values above 2.5 AU), the samples were diluted with an appropriate volume of phosphate buffer. The blank was measured using 200 µL of phosphate buffer. Subsequently, to determine the total TPA content of the analysed samples, the average value (ϵ) of the three extinction coefficients (Fig. 3a and Supplementary Fig. S8) (or the reported value⁴¹ in case of the A₂₆₀ measurements) was used.

LCC-mediated enzymatic degradation of PET films

7 mg of commercial PET film was incubated in 1 mL phosphate buffer (100 mM K₂HPO₄ – KH₂PO₄, pH 8.0) containing 10 µg of purified LCC. The reaction mixture was incubated at 65 °C, at 700 rpm in an Eppendorf ThermoMixer C. Samples were taken at various reaction times, from 1 to 114 h and analysed by HPLC or UV-absorbance measurements as described in Section “[Enzymatic activity assessment by HPLC](#)” and Section “[Enzymatic activity assessment by UV-spectroscopy](#)”, respectively.

Results and discussion

Several published HPLC methods, employed for the analysis of PET-hydrolysis products (Fig. 1a), determine the overall TPA content (including also TPA equivalents calculated from the MHET and BHET contents) by calibration curves based on the integration of the peak areas of the three different aromatic PET-degradation products^{20,25,27}. To increase the precision and accuracy of the HPLC method, we tested the use of caffeine as the internal standard. The simultaneous measurement of the analyte(s) of interest and of the internal standard, added at known concentration and in equal amount to all analyzed samples, reduces the deviation within the quantitative assessments of the analyte's concentration. The potential differences among the sample preparation and analysis provide similar changes to the internal standard's signal as to those occurring in the analyte's signal intensities. Therefore, a calibration curve exhibiting the relationship between the *ratios* of the internal standard's and analyte's signals versus their corresponding concentrations, diminishes the effect of modifications in analyte/analysis conditions on the peak area of individual signals. Accordingly, compared to the quantification of individual signals, the use of internal standard provides a more accurate determination of the analyte's concentration^{41,42}. The high accessibility of caffeine, its inertness towards PET and enzymatic PET-degradation products, its highly efficient separation by HPLC procedures from other aromatic compounds, good quantifiability and its linear response range between 0.1625 and 0.4875 mg/mL^{43–45} have been the starting point for its use as internal standard. The polar functional groups and aromatic moiety of caffeine, similar to those of TPA, MHET, and BHET, enabled its retention and elution by reverse-phase HPLC. At the same time, its structural differences provided caffeine a distinct retention time from those of PET-degradation products and facilitated its reliable detection and efficient separation from the reaction products (Fig. 1b and Supplementary

Fig. S4). Resolution is a crucial parameter during HPLC method development, a major driving force being the reach of high resolution in short elution times. A resolution value > 1.5 between two consecutive peaks ensures that the sample components are well separated (baseline separation) and enable precise determination of each peak's area. In the developed HPLC method (Fig. 1b), the highest resolution value was 9.64, while the lowest value between two consecutive peaks was 3.99 (Supplementary Table S3), near an elution time less than 10 minutes, demonstrating its further applicability for quantitative measurements.

For quantitative assessments, using the authentic samples of caffeine and the three aromatic products of the PET-hydrolysis (TPA, MHET and BHET), and a reverse-phase HPLC method with baseline separation of each component (Fig. 1b and Supplementary Fig. S5), we provided calibration curves allowing quantification of each individual aromatic product of the enzymatic PET-hydrolysis (Fig. 2). To minimize the influence of the sample matrix on the analyte's signal, we ensured that the calibrator samples shared identical composition with the samples taken from the enzymatic reaction. Since acetonitrile is used to stop the enzyme's activity within the samples taken from the PET-degradation reaction, therefore within the calibration samples a constant v/v ratio of 1:1 of the phosphate reaction buffer and acetonitrile was maintained, as within the analyzed reaction samples. The concentration range, from approximately 21 μM to 1.69 mM (of each aromatic component), covered by the calibration curves, enables the assessment of highly active and also less efficient PET-degrading enzyme variants. For instance, using the LCC variants^{42,46} or FAST-PETase under destabilization conditions^{25,42,46}, the reported product concentration was $\sim 500 \mu\text{M}$ and $\sim 200 \mu\text{M}$, respectively, which is well within the concentration range covered by our calibration curves. In case if the measured quantity of the overall product, generally assessed as TPA equivalent^{2,3,21,26,29,38–41}, comprising besides the TPA concentration also the MHET and BHET content (in TPA_{eq}), exceeds the concentration range of the calibration curve, sample dilution can be applied. The level of baseline noise was of 5.73 mAU, while its 3-fold extension revealed a limit of detection of 17.20 mAU, equivalent to 0.49 μM of TPA, 0.40 μM of MHET and 0.21 μM of BHET. These product concentrations are at least ~ 400 -fold lower than the reported content of PET-degradation products, mentioned above in case of the PET-degrading enzyme variants^{25,42,46}, thus supporting the applicability of our method for monitoring the PET degradation reaction.

Within the linear regression model, the calibration curve on the entire concentration range, showed a coefficient of determination of $R^2_{\text{TPA}} = 0.9939$ (Supplementary Fig. S6a), $R^2_{\text{MHET}} = 0.9879$ (Supplementary Fig. S6b), $R^2_{\text{BHET}} = 0.9961$ (Supplementary Fig. S6c) with a slight break of linearity. By splitting the calibration curves for lower and higher concentrations, the accuracy and reliability slightly increased, with $R^2 > 0.999$ in all cases (Fig. 2a and b). The average slopes of the calibration curves obtained for the separated concentration ranges, exhibit a difference, e.g. in case of BHET concentration exceeding 19%, when compared to the values obtained for the total concentration range (Supplementary Table S4), further justifying the separation of the curves.

To test and compare the reproducibility and the accuracy of the developed method with the previously employed HPLC methods, we analyzed a particular sample with defined TPA, MHET and BHET content over three different days. In each day three measurements were performed, representing three technical replicates, yielding the measured concentration (C_{measured}) for each day and the average concentration ($\bar{C}_{\text{measured}}$) across the three days. As Table 1 indicates, the standard deviation values (STD) among the technical replicates were in all cases higher for the HPLC method lacking the internal standard, referred here as the conventional method (HPLC_{conv.}). In some cases, such as the determination of MHET concentration on day 3, the STD of the conventional method was > 10 -fold higher than the one registered for the internal standard method and reached an unacceptable 46% of the determined concentration value. For the TPA content measured on day 1 and 2, the STD values of the conventional method (HPLC_{conv.}), were > 2 -fold higher compared to the values determined by the novel method.

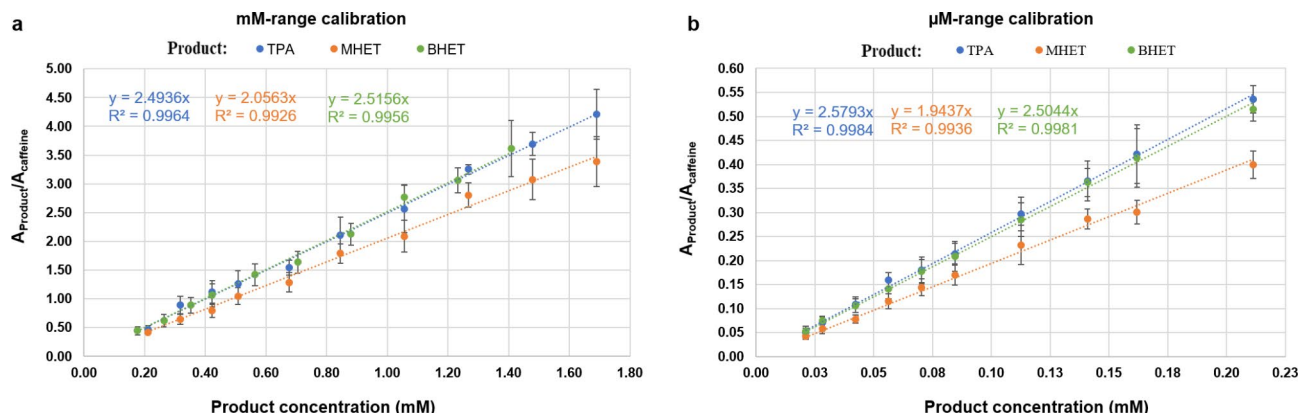


Fig. 2. Calibration curves for the different concentration domains of the PET-hydrolysis products, obtained by representing the ratios of peak areas specific to each product and caffeine as a function of the molar concentration of the products: (a) calibration curve for the high, mM-concentration range (0.176–1.690 mM) of the products; (b) calibration curve for the low, μM -concentration range (21–211 μM) of the products.

		$C_{measured}$ (mM)	\pm STD	$\bar{C}_{measured}$ (mM)	$C_{theoretical}$ (mM)	Error* (%)	CV (%)	Accuracy (%)	Precision (%)
TPA									
$HPLC_{int,std.}$	Day 1	1.423	0.05	1.348	1.268	6.30	3.80	93.70	5.12
	Day 2	1.279	0.13				9.86		13.28
	Day 3	1.341	0.17				12.51		16.86
$HPLC_{conv.}$	Day 1	1.089	0.15	1.136	1.268	10.36	13.01	89.64	14.78
	Day 2	1.326	0.31				26.83		30.49
	Day 3	0.994	0.21				18.12		20.59
MHET									
$HPLC_{int,std.}$	Day 1	1.281	0.02	1.184	1.268	6.57	1.71	93.43	2.02
	Day 2	1.103	0.10				8.32		9.64
	Day 3	1.169	0.05				4.43		5.24
$HPLC_{conv.}$	Day 1	0.788	0.07	0.974	1.268	23.20	7.05	76.81	6.86
	Day 2	0.898	0.02				1.50		1.46
	Day 3	1.235	0.57				58.83		57.28
BHET									
$HPLC_{int,std.}$	Day 1	1.042	0.03	1.004	0.986	1.79	3.40	98.21	3.41
	Day 2	0.950	0.09				8.52		8.55
	Day 3	1.018	0.01				1.43		1.44
$HPLC_{conv.}$	Day 1	0.717	0.10	0.763	0.986	22.56	12.59	77.44	9.61
	Day 2	0.818	0.06				7.57		5.78
	Day 3	0.756	0.12				15.16		11.78

Table 1. Assessed concentrations of TPA, MHET and BHET and analytical parameters obtained from the analysis of the control sample, with TPA, MHET and BHET content fixed by weighting the authentic samples, on three different days (in triplicate in each day) using both the conventional ($HPLC_{conv.}$) and the herein developed internal standard ($HPLC_{int,std.}$) HPLC methods. *The error value represents the difference between the average measured concentration and the theoretical value calculated based on the pipetted volume of standard samples, relative to the latter. For the detailed description of formulas used for calculation of the analytical parameters see Supplementary materials, Sect. 4.2)

To further validate the novel method, additional performance parameters, such as coefficient of variation (CV), accuracy and precision were also determined (Table 1). The coefficient of variation (CV) is a dimensionless value, appropriate for comparing two data sets based on the degree of variation. It is defined as the ratio of standard deviation to the mean value and should be < 20% for a method to be accepted⁴⁷. The internal standard method developed by us showed considerably lower variations, with CV values ranging from 1.43 to 12.51, whereas the conventional method showed significantly higher coefficients of variation, up to 58.83. Accuracy, expressed as a percentage, is determined by subtracting the calculated error values from 100⁴⁸ and indicates the proximity of measured values to the theoretical ones. In this case the theoretical values were the theoretical concentrations ($C_{theoretical}$) of the three analytes, TPA, MHET, BHET, controlled within the analyzed sample by weighting from their authentic samples. In case of MHET and BHET, the conventional method ($HPLC_{conv.}$) exhibited significantly higher errors (> 22%) compared to the values provided by the internal standard method ($HPLC_{int,std.}$), which presented only 6.6% and 1.8% deviation, respectively, from the ‘real’ MHET and BHET concentrations of the sample. Regarding TPA, the novel method showed ~ 6% deviation from the set-up TPA concentration in comparison with the ~ 10% error of the conventional method. Accordingly, the accuracy of our internal standard method exceeded 93.4% in case of each PET-degradation product. At the same time, the conventional method achieved its highest accuracy of 89.6% in case of TPA content determinations, with accuracy values of only 76.8% and 77.4% for MHET and BHET, respectively. Consequently, the precision of the method, expressed as a percentage of the standard deviation, was also superior for the internal standard-containing HPLC method, with the lowest value of 1.4% being registered in case of BHET content determinations. These results highlight that procedures based solely on the determination of the absolute value of the peak area specific to each individual product are subjected to peak area variations among the multiple injections of the same sample, which contributes to their higher error, low accuracy and precision values (Table 1). In contrast, the internal standard method using ratios of peak areas normalized to the peak area of the internal standard, employed in constant concentration, minimizes the overall calculation error, since any factor influencing the peak area of the analyte affects also that of the internal standard.

The second most predominantly employed monitoring method for enzymatic PET-hydrolysis is based on UV-spectroscopy. Within this bulk absorbance method⁴¹, the absorbance value of the aromatic PET-degradation products – TPA, MHET and BHET – is registered at the wavelength of 260 nm, while for quantifications the medium extinction coefficient derived only from the individual coefficients of MHET and of TPA have been employed. In our experiments, the absorbance scan of the three aromatic PET-degradation products, at their identical concentrations of 0.1 mM, presented significant variation of their absorbance intensities at 260 nm

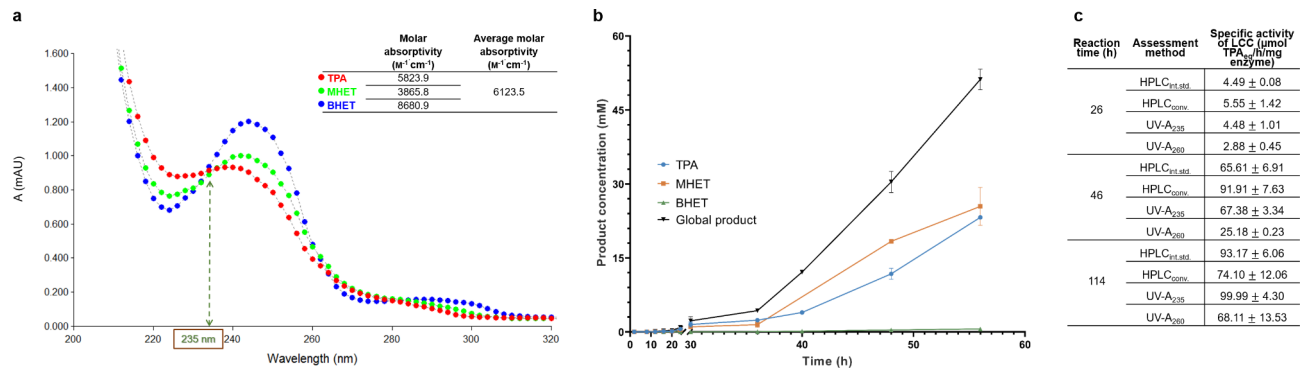


Fig. 3. Upgrading the UV-method and monitoring the progression of the LCC-catalyzed PET-hydrolysis. (a) Overlay UV absorbance spectra of terephthalic acid (TPA), mono-(2-hydroxyethyl) terephthalic acid (MHET) and bis-(2-hydroxyethyl) terephthalate (BHET) and their molar absorptivity determined at 235 nm. (b) Monitoring the concentration of each individual product BHET, MHET, TPA and of the global TPA content, during the LCC-mediated enzymatic hydrolysis of the commercial PET film, using the improved internal standard containing HPLC method. (For reaction conditions please see Section “[LCC-mediated enzymatic degradation of PET films in the Experimental part](#)”) (c) Specific PET-hydrolysis activity of the recombinant leaf-branch compost cutinase (LCC) determined by the conventional (HPLC_{conv.}) and internal standard-containing (HPLC_{int.std.}) HPLC methods and by the reported UV-spectroscopy method (UV-A₂₆₀) or the herein optimized UV-method (UV-A₂₃₅).

(Fig. 3a). Accordingly, determining the TPA_{eq} content by using the medium extinction coefficient determined at 260 nm might lead to an under- or overestimation of the TPA_{eq}, the extent of which depends on the molar percentage of the different products within the analysed sample. Based on the obtained overlaid absorbance spectra (Fig. 3a) of TPA, MHET and BHET, we selected 235 nm as optimal wavelength for product monitoring. The mean extinction coefficient was determined from the three extinction coefficients (Fig. 3a), assessed by using authentic samples of each product (TPA, MHET, and BHET – Supplementary Fig. S8c). Since, the average molar absorptivity positions close (~5% higher) to those of TPA, the method is likely to be highly accurate for samples with large molar content of TPA. However, for samples with large MHET and BHET content, the 37% and 42% difference, respectively, between the average molar absorptivity and those of BHET and MHET, might lead to increased errors in the quantification of the global TPA content, provided by these bulk-absorbance methods.

For validation of the developed methods, we monitored the PET-degrading activity of the recombinant leaf-branch compost cutinase (LCC), reported as one of the most efficient PET-degrading enzymes^{29,30,35,42}. The recombinant LCC enzyme was cloned and purified using a previously described method²⁹, while its activity was assessed employing the recently published optimized reaction conditions⁴⁶. The specific activity of the wild-type enzyme was monitored utilizing both HPLC methods tested above (HPLC_{conv.} and HPLC_{int.std.}). Additionally, to cross-validate the activity values, the reported UV-spectroscopy method⁴¹ and its herein optimized variant were also employed for activity measurements, serving as further comparative basis. The activity of the recombinant LCC, determined by the internal standard HPLC method was ~66 (μmol TPA_{eq}/h/mg enzyme) and ~93 (μmol TPA_{eq}/h/mg enzyme), after 46- and 114-hours reaction time, respectively (Fig. 3b and c). These values are similar to the reported values of ~72 (μmol TPA_{eq}/h/mg enzyme)²⁷ after 24 h of reaction time, while somewhat higher than the recently reported specific activities of ~17.31 (μmol TPA_{eq}/h/mg enzyme) and ~11.96 (μmol TPA_{eq}/h/mg enzyme) after 26- and 46-h reaction time⁴².

Interestingly, the LCC activity of ~4.48 (μmol TPA_{eq}/h/mg enzyme), ~67.38 (μmol TPA_{eq}/h/mg enzyme) and ~99.99 (μmol TPA_{eq}/h/mg enzyme) after 24, 46 and 114 h reaction time, respectively, measured by our improved UV-spectroscopy method, highly resembled the activity values determined by the internal standard HPLC procedure (~4.49 μmol TPA_{eq}/h/mg enzyme, ~65.61 μmol TPA_{eq}/h/mg enzyme and ~93.17 μmol TPA_{eq}/h/mg enzyme; see Fig. 3c). Accordingly, the optimized bulk absorbance method provides a facile alternative for the precise determination of the TPA content of the product mixture obtained from the PET degradation. In contrast, the reported bulk-absorbance procedure (UV-A₂₆₀) provided an activity value of ~25 (μmol TPA_{eq}/h/mg enzyme) after 46-hours reaction time (Fig. 3c), representing a sub-estimation of 61.6% and 72.6% of the total TPA content measured by the internal standard-based and conventional HPLC methods, respectively.

Finally, we monitored the efficiency of the PET-hydrolysis (Supplementary Fig. S10) over an extended period of 56 h, providing the time-productivity profile of the reaction (Fig. 3b). The results showed high similarities to recently published data, with 25 mM product concentration (as TPA_{eq}) reported after 50 h of reaction time⁴², while in our case in same reaction time 36 mM TPA_{eq} concentration was determined. The reported reactions also exhibit a lag period (with low productivity in time) for the experiments performed at 60 °C or below, followed by a significant productivity increase, similar to our case. The increased lag period, also present in our experiments, might be due to the known issues related to the influence of the crystallinity degree of the PET film. Excluding the initiation / lag-time, after ~40-hour reaction time, the product concentration reached ~650 μM

(Fig. 3c), the specific activity values of LCC approaching the reported data^{25,42,46}. Notably, our developed internal standard-based HPLC method also enables the quantification of the individual distribution of TPA, MHET and BHET over the reaction time (Fig. 3b), providing detailed product distribution profile of the PET-hydrolysis reaction.

Conclusions

The precise monitoring of enzymatic PET-hydrolysis and the relative content of the different degradation products is of high interest in developing novel biocatalysts for the efficient PET-degradation and recycling. Within this study, the methods used for monitoring the enzymatic PET-degradation have been significantly improved in terms of accuracy. Using caffeine as internal standard we provided an improved HPLC method, that besides the increased accuracy in the assessment of the overall TPA content, also allowed the determination of the molar distribution and the relative content of each aromatic reaction product of the enzymatic PET-hydrolysis, namely TPA, MHET, BHET. The established calibration curves cover a broad concentration range (from the μM to low mM scale) of the PET-hydrolysis products. Therefore, the method is suitable for assessing both low and high PETase activities, having a limit of detection ~ 400-fold below the reported PET-degrading activities of LCC and FAST-PETase, two of the best performing PET-hydrolases. This internal standard-based HPLC method, when compared to previously employed methods, provided lower dispersion of product concentrations from multiple measurements, lower deviations from theoretical values, lower degrees of variation and of errors and higher accuracy as well. The HPLC method was also employed for monitoring the progress of the PET-hydrolysis reaction catalysed by LCC, in which case the assessed global TPA content was similar to the reported values. Additionally, to the reported data, our method enabled the determination of the individual time-productivity profile of each aromatic reaction product, demonstrating its high utility in monitoring the enzymatic PET-hydrolysis.

Besides, the second most predominantly employed UV-Vis bulk absorbance method was also improved and used for cross-validating the activity values obtained with the improved HPLC method. The specific activity values of the LCC provided by the two methods were highly similar, in contrast to the values provided by the known UV-assay, supporting the superiority of the herein fine-tuned UV-procedure to the previously reported spectrophotometric methods.

Accordingly, by revisiting and optimizing HPLC and UV-spectroscopy methods, herein we provide two facile analytical assays for the accurate monitoring of the enzymatic PET-hydrolysis. At the same time, the developed HPLC method allows the assessment of individual time-productivity profiles for each aromatic PET-degradation product.

Data availability

The GenBank and Uniprot identifiers for the gene and protein sequence of the leaf-branch compost cutinase (LCC) used within the experimental work are GenBank ID: HQ704839.1, UniProt ID: G9BY57, respectively and are also described within the manuscript and supplementary data, while other datasets used or analysed during the current study are available from the corresponding author on reasonable request.

Received: 14 July 2024; Accepted: 20 December 2024

Published online: 13 January 2025

References

- Dhaka, V. et al. Occurrence, toxicity and remediation of polyethylene terephthalate plastics. A review. *Environ. Chem. Lett.* **20**, 1777–1800. <https://doi.org/10.1007/s10311-021-01384-8> (2022).
- Son, H. F. et al. Structural bioinformatics-based protein engineering of thermo-stable PETase from Ideonella sakaiensis. *Enzyme Microbiol. Technol.* **141**, 1–8. <https://doi.org/10.1016/j.enzmictec.2020.109656> (2020).
- Austin, H. et al. Characterization and engineering of a plastic-degrading aromatic polyesterase. *Proc. Natl. Acad. Sci. USA.* **115**, 4350–4357. <https://doi.org/10.1073/pnas.1718804115> (2018).
- Annual Report. 2021 of Plastic Soup Foundation https://www.plasticsoupfoundation.org/wp-content/uploads/2022/09/PSF_ANNUAL-REPORT_2021_EN.pdf
- Plastics Europe. The Circular Economy for Plastics – A European Overview 2022, <https://plasticseurope.org/knowledge-hub/the-circular-economy-for-plastics-a-european-overview-2/>
- Geyer, R., Jambeck, J. R. & Law, K. L. Production, use, and fate of all plastics ever made. *Sci. Adv.* **3**, e1700782. <https://doi.org/10.1126/sciadv.1700782> (2017).
- Jambeck, J. R. et al. Plastic waste inputs from land into the ocean. *Science* **347**, 768–771. <https://doi.org/10.1126/science.1260352> (2015).
- MacLeod, M., Arp, H. P. H., Tekman, M. B. & Jahnke, A. The global threat from plastic pollution. *Science* **373**, 61–65 (2021).
- Xu, L. et al. Missing relationship between meso- and microplastics in adjacent soils and sediments. *J. Hazard. Mater.* **424**, 127234–127244. <https://doi.org/10.1016/j.jhazmat.2021.127234> (2022).
- Courtene-Jones, W., Quinn, B., Gary, S. F., Mogg, A. O. M. & Narayanaswamy, B. E. Microplastic pollution identified in deep-sea water and ingested by benthic invertebrates in the Rockall Trough, North Atlantic Ocean. *Environ. Pollut.* **231**, 271–280. <https://doi.org/10.1016/j.envpol.2017.08.026> (2017).
- Nizzetto, L., Futter, M. & Langas, S. Are agricultural soils dumps for microplastics of urban origin? *Environ. Sci. Technol.* **50**, 10777–10779. <https://doi.org/10.1021/acs.est.6b04140> (2016).
- Enyoh, C. E., Verla, A. W., Ibe, F. C. & Amaobi, C. E. Airborne microplastics: a review study on method for analysis, occurrence, movement and risks. *Environ. Monit. Assess.* **191**, 668–685. <https://doi.org/10.1007/s10661-019-7842-0> (2019).
- Waller, C. L. et al. Microplastics in the Antarctic Marine system: an emerging area of research. *Sci. Total Environ.* **598**, 220–227. <https://doi.org/10.1016/j.scitotenv.2017.03.283> (2017).
- Waring, R. H., Harris, R. M. & Mitchell, S. C. Plastic contamination of the food chain: A threat to human health? *Maturitas* **115**, 64–68, (2018). <https://doi.org/10.1016/j.maturitas.2018.06.010>
- Leslie, H. A. et al. Discovery and quantification of plastic particle pollution in human blood. *Environ. Int.* **163**, 107199–107207. <https://doi.org/10.1016/j.envint.2022.107199> (2022).

16. Schyns, Z. O. G. & Shaver, M. P. Mechanical recycling of packaging plastics: a review. *Macromol. Rapid Commun.* **42**, 120–147. <https://doi.org/10.1002/marc.202000415> (2021).
17. Thachnatharen, N., Shahabuddin, S. & Sridewi, N. The waste management of polyethylene terephthalate (PET) plastic waste: a review. *IOP Conf. Ser. : Mater. Sci. Eng.* **1127**, 12002–12009. <https://doi.org/10.1088/1757-899x/1127/1/012002> (2021).
18. Carbios – Biotechnology powering plastic and textile circularity. <https://www.carbios.com/en>
19. Thiagarajan, S., Maaskant-Reilink, E., Ewing, T. A., Julsing, M. K. & van Haveren, J. Back-to-monomer recycling of polycondensation polymers: opportunities for chemicals and enzymes. *RSC Adv.* **12**, 947–970. <https://doi.org/10.1039/d1ra08217e> (2021).
20. Müller, R. J., Schrader, H., Profe, J., Dresler, K. & Deckwer, W. D. Enzymatic degradation of poly(ethylene terephthalate): rapid hydrolyse using a hydrolase from *T. Fusca*. *Macromol. Rapid Commun.* **26**, 1400–1405. <https://doi.org/10.1002/marc.200500410> (2005).
21. Sagong, H. Y. et al. Decomposition of the PET Film by MHETase using Exo-PETase function. *ACS Catal.* **10**, 4805–4812. <https://doi.org/10.1021/acscatal.9b05604> (2020).
22. Wei, R. et al. Biocatalytic degradation efficiency of postconsumer polyethylene terephthalate packaging determined by their polymer microstructures. *Adv. Sci. (Weinh.)* **6**, 1900491–1900501. <https://doi.org/10.1002/advs.201900491> (2019).
23. Kawai, F., Kawabata, T. & Oda, M. Current knowledge on enzymatic PET degradation and its possible application to waste stream management and other fields. *Appl. Microbiol. Biotechnol.* **103**, 4253–4268. <https://doi.org/10.1007/s00253-019-09717-y> (2019).
24. Yoshida, S. et al. A bacterium that degrades and assimilates poly(ethylene terephthalate). *Science* **351**, 1196–1199. <https://doi.org/10.1126/science.aad6359> (2016).
25. Joo, S. et al. Structural insight into molecular mechanism of poly(ethylene terephthalate) degradation. *Nat. Commun.* **9**, 382–394. <https://doi.org/10.1038/s41467-018-02881-1> (2018).
26. Son, H. F. et al. Rational protein Engineering of Thermo-stable PETase from *Ideonella sakaiensis* for highly efficient PET degradation. *ACS Catal.* **9**, 3519–3526. <https://doi.org/10.1021/acscatal.9b00568> (2019).
27. Sulaiman, S. et al. Isolation of a novel cutinase homolog with polyethylene terephthalate-degrading activity from leaf-branch compost by using a metagenomic approach. *Appl. Environ. Microbiol.* **78**, 1556–1562. <https://doi.org/10.1128/AEM.06725-11> (2012).
28. Zhu, B., Ye, Q., Seo, Y. & Wei, N. Enzymatic degradation of polyethylene terephthalate plastics by bacterial curli display PETase. *Environ. Sci. Technol. Lett.* **9**, 650–657. <https://doi.org/10.1021/acs.estlett.2c00332> (2022).
29. Tournier, V. et al. An engineered PET depolymerase to break down and recycle plastic bottles. *Nature* **580**, 216–219. <https://doi.org/10.1038/s41586-020-2149-4> (2020).
30. Pirillo, V., Pollegioni, L. & Molla, G. Analytical methods for the investigation of enzyme-catalyzed degradation of polyethylene terephthalate. *FEBS J.* **288**, 4730–4745. <https://doi.org/10.1111/febs.15850> (2021).
31. The United States Pharmacopeia, USP 29. USP Convention, <661> plastic packaging systems and their materials of construction. 2655–2663 (2006).
32. Spitz, H. D. & Weinberger, J. Determination of ethylene oxide, ethylene chlorohydrin, and ethylene glycol by gas chromatography. *J. Pharm. Sci.* **60**, 271–274. <https://doi.org/10.1002/jps.2600600225>
33. Tran, B. N., Okoniewski, R., Bucciferro, A., Jansing, R. & Aldous, K. M. Determination of trace amounts of ethylene glycol and its analogs in water matrixes by liquid chromatography/tandem mass spectrometry. *J. AOAC Int.* **97**, 232–237. <https://doi.org/10.5740/jaacint.12-198> (2014).
34. Perez Medina Martinez, V., de la Espinosa, C. E., Hernandez-Garcia, A. G. & Perez, N. O. Detection and quantification of leached ethylene glycol in biopharmaceuticals by RP-UHPLC. *Anal. Bioanal. Chem.* **412**, 1795–1806. <https://doi.org/10.1007/s00216-020-02425-x> (2020).
35. Wei, R., Oeser, T., Billig, S. & Zimmermann, W. A high-throughput assay for enzymatic polyester hydrolysis activity by fluorimetric detection. *Biotechnol. J.* **7**, 1517–1521. <https://doi.org/10.1002/biot.201200119> (2012).
36. Halonen, P., Reinikainen, T., Nyssölä, A. & Buchert, J. A high throughput profiling method for cutinolytic esterases. *Enzyme Microb. Technol.* **44**, 394–399. <https://doi.org/10.1016/j.enzmictec.2008.12.012> (2009).
37. Vogel, K. et al. Enzymatic degradation of polyethylene terephthalate nanoplastics analyzed in real time by isothermal titration calorimetry. *Sci. Total Environ.* **773**, 145111–145121. <https://doi.org/10.1016/j.scitotenv.2021.145111> (2021).
38. Meng, X. et al. Protein engineering of stable IsPETase for PET plastic degradation by Premuse. *Int. J. Biol. Macromol.* **180**, 667–676. <https://doi.org/10.1016/j.ijbiomac.2021.03.058> (2021).
39. Seo, H. et al. Reply to conformational fitting of a flexible oligomeric substrate does not explain the enzymatic PET degradation. *Nat. Commun.* **10**, 5582–5583. <https://doi.org/10.1038/s41467-019-13493-8> (2019).
40. Palm, G. J. et al. Structure of the plastic-degrading *Ideonella sakaiensis* MHETase bound to a substrate. *Nat. Commun.* **10**, 1–10. <https://doi.org/10.1038/s41467-019-09326-3> (2019).
41. Zhong-Johnson, E. Z. L., Voigt, C. A. & Sinskey, A. J. An absorbance method for analysis of enzymatic degradation kinetics of poly(ethylene terephthalate) films. *Sci. Rep.* **11**, 1–9. <https://doi.org/10.1038/s41598-020-79031-5> (2021).
42. Pirillo, V., Orlando, M., Battaglia, C., Pollegioni, L. & Molla, G. Efficient polyethylene terephthalate degradation at moderate temperature: a protein engineering study of LC-cutinase highlights the key role of residue 243. *FEBS J.* **290**, 3185–3202. <https://doi.org/10.1111/febs.16736> (2023).
43. Acheampong, A., Gyasi, W. O., Darko, G., Apau, J. & Addai-Arhin, S. Validated RP-HPLC method for simultaneous determination and quantification of chlorpheniramine maleate, Paracetamol and caffeine in tablet formulation. *Springerplus* **5**, 625. <https://doi.org/10.1186/s40064-016-2241-2> (2016).
44. Fekry, R. A., Kelani, K. M., Fayed, Y. M. & Tantawy, M. A. Comparative validated chromatographic methods for the simultaneous determination of caffeine, codeine, Paracetamol along with the related compound p-aminophenol in tablets. *JPC – J. Planar Chromatogr. - Mod. TLC.* **35**, 51–59. <https://doi.org/10.1007/s00764-022-00150-y> (2022).
45. Ismail, A., Gamal, M. & Nasr, M. Optimization of analytical method for simultaneous determination of acetaminophen, caffeine, and aspirin in tablet dosage form. *Pharm. Chem. J.* **56**, 1682–1688. <https://doi.org/10.1007/s11094-023-02844-x> (2023).
46. Arnal, G. et al. Assessment of four engineered PET degrading enzymes considering large-scale industrial applications. *ACS Catal.* **13**, 13156–13166. <https://doi.org/10.1021/acscatal.3c02922> (2023).
47. Iversen, P. W., Beck, B. & Chen, Y. F. HTS assay validation, <https://www.ncbi.nlm.nih.gov/books/NBK83783/>
48. Huber, L. Validation of analytical methods. (2010).

Acknowledgements

K.B. and B.E.N. thanks the support of the Collegium Talentum Programme of Hungary. B.E.N. thanks the STAR-Institute of the Babeş-Bolyai University for the provided student-research fellowship. K.B. and R.B.T. thanks the STAR-Institute of the Babeş-Bolyai University for the provided doctoral advanced fellowships (contract nr. 21PFE/ 30.12.2021, ID: PFE-550-UBB).

Author contributions

K.B. and B.E.N. were responsible for investigation, methodology, data curation related to HPLC, UV-spectros-

copy measurements, and prepared the original draft of the manuscript. K.B. and R.B.T were responsible for investigation, methodology related to the cloning and purification of LCC. R.T. was involved in the development/optimization of the HPLC method. L.C.B. was responsible for conceptualization, data curation and for supervising all experiments. M.I.T., C.P. and L.C.B. were responsible for funding acquisition and for writing the manuscript. All authors reviewed the manuscript.

Declarations

Competing interests

The authors declare no competing interests.

Additional information

Supplementary Information The online version contains supplementary material available at <https://doi.org/10.1038/s41598-024-84177-7>.

Correspondence and requests for materials should be addressed to L.C.B.

Reprints and permissions information is available at www.nature.com/reprints.

Publisher's note Springer Nature remains neutral with regard to jurisdictional claims in published maps and institutional affiliations.

Open Access This article is licensed under a Creative Commons Attribution-NonCommercial-NoDerivatives 4.0 International License, which permits any non-commercial use, sharing, distribution and reproduction in any medium or format, as long as you give appropriate credit to the original author(s) and the source, provide a link to the Creative Commons licence, and indicate if you modified the licensed material. You do not have permission under this licence to share adapted material derived from this article or parts of it. The images or other third party material in this article are included in the article's Creative Commons licence, unless indicated otherwise in a credit line to the material. If material is not included in the article's Creative Commons licence and your intended use is not permitted by statutory regulation or exceeds the permitted use, you will need to obtain permission directly from the copyright holder. To view a copy of this licence, visit <http://creativecommons.org/licenses/by-nc-nd/4.0/>.

© The Author(s) 2025